UDC 551.511.2:551.558.2

Note on Design of an Optimized Computation Scheme For Kinematic Vertical Motion Fields[1,2]

ERNEST C. KUNG—*Department of Atmospheric Science, University of Missouri, Columbia, Mo.*

ABSTRACT—The design of an optimized computation scheme for kinematic vertical motion fields with an upper air network is discussed with a scheme that incorporates 14 degrees of optimization in the evaluation of divergence. The provided range of optimization enables the computation scheme to suit wide varieties of data dispostion in the observation network, and the well-known problem of bias error accumulation in the kinematic ω profiles seems to have been practically overcome. The discussions include the general construction of the scheme in terms of the sequential flow of the computation, the quality of the vertical motion field over the synoptic network through the depth of the atmosphere, and the utilization and application of the scheme under various circumstances.

1. INTRODUCTION

As an integral part of our observational study of atmospheric energetics, the development of a scheme for the kinematic estimate of the vertical motion field is under way. Since it is based on no assumptions about the nature of the atmospheric circulation except the hydrostatic relationship, the kinematic estimate of the vertical p velocity, ω, has paramount importance in the objective energy diagnosis.

In a preceding paper (Kung 1972), a new approach to the kinematic estimate of the vertical motion field with an upper air network was presented. The scheme has been designed under the presumption that the vertical profile of ω should converge to a near-zero value at the top of the atmosphere without being so required when a sensitive balance between the analysis scheme and the data disposition is achieved. Thus, a range of optimization is provided in a computation scheme to suit wide varieties of data disposition in the observation network. The preliminary computation with eight degrees of optimization in a scheme, as reported in the previous paper, has supported this presumption, and our extensive computational studies subsequent to the paper also confirm the approach. Thus, it may be concluded that the well-known problem of bias error accumulation in the kinematic ω profiles can be practically overcome, and meaningful fields of kinematic vertical p velocity can be obtained through the depth of the atmosphere with observed wind data over a large synoptic upper air network.

Since the publication of our last report (Kung 1972), the scheme has been improved to include 14 degrees of optimization as a result of our continued experiment in the numerical analysis. Currently, a comprehensive energy diagnosis is in progress with aerological data over North America and other areas of the Northern Hemisphere, which incorporates the computation of the vertical motion field with the 14-degree optimization method. The principles of this particular optimization method are also being applied to analyses of special observation networks data to study the problems of subsynoptic scale energy transformations and tropical energy conversions. The results of those energy analyses will be reported in separate papers. The purpose of this contribution is to describe the 14-degree optimization scheme as our basic computation scheme for kinematic ω fields and to comment on the nature and use of derived ω fields from the utility point of view. We have been receiving comments and inquiries concerning the subsequent development and application of the scheme since the publication of our last report, and we hope that this note will also serve the interested audience in that respect. For the conceptual discussion of the approach, the reader is referred to our last report.

2. FOURTEEN-DEGREE OPTIMIZATION SCHEME

With the standard notations for the hemispheric polar coordinate (x,y,p,t) system, the vertical p velocity is defined as

$$\omega=\frac{dp}{dt} \tag{1}$$

and the continuity equation takes the form

$$\nabla\cdot\mathbf{V}+\frac{\partial\omega}{\partial p}=0. \tag{2}$$

Designating ω_{p_1} and ω_{p_2} as ω at pressure levels p_1 and p_2, we may obtain ω_{p_1} by vertically integrating the continuity equation; that is,

$$\omega_{p_1}=\omega_{p_2}+\int_{p_1}^{p_2}\nabla\cdot\mathbf{V}dp, \tag{3}$$

provided ω_{p_2} has been specified or has already been obtained by integrating the continuity equation to the pressure level p_2. At the surface level, ω may be assumed

[1] This research was supported by the Atmospheric Science Section, National Science Foundation, under NSF Grant GA-15952.

[2] Contribution from the Missouri Agricultural Experiment Station, Journal Series No. 6647

to be 0 when a large-scale network is utilized for data input. The divergence of the horizontal wind is to be obtained with the observed wind data as

$$\nabla\cdot\mathbf{V}=\frac{1}{R\cos\phi}\frac{\partial u}{\partial\lambda}+\frac{1}{R\cos\phi}\frac{\partial(v\cos\phi)}{\partial\phi} \tag{4}$$

where R is the mean radius of the earth, γ is the longitude, and ϕ is the latitude.

The evaluation of horizontal derivatives of the wind components, the interpolation of missing wind data, and some space smoothing of the computed divergence for certain degrees of optimization make use of the polynomial representation of a scalar field either with the quadratic surface equation,

$$P(\lambda,\ )=\phi r_1\lambda^2+r_2\lambda+r_3\lambda\phi+r_4\phi+r_5\phi^2+r_6, \tag{5}$$

or with the plane surface equation,

$$P(\lambda,\phi)=s_1\lambda+s_2\phi+s_3, \tag{6}$$

where $P(\lambda,\phi)$ is a dummy scalar variable, and r and s are coefficients to be determined with at least six or three values of P, respectively.

The commonly recognized bias errors that accumulate in computing ω are mainly introduced in values of $\nabla\cdot\mathbf{V}$ through either the wind observation or the evaluation of the horizontal derivatives of the wind components. Thus, the optimization of the computation scheme of ω is accomplished by optimizing the process to evaluate the divergence, $\nabla\cdot\mathbf{V}$. The sequential operation of the 14-degree optimization scheme to compute ω is described as follows.

Interpolation of Missing Wind Data

After wind data over a synoptic network at an observation time are read in, a scan is made for stations with missing data. If a station with missing data is surrounded by three or more nearby stations with available data, interpolation of the u and v components of wind is made separately to the missing data station, utilizing the surrounding stations. In the case of three available surrounding stations, the exact fitting of the plane surface with eq (6) is used. In the case of four to six available stations, the least squares fitting with eq (6) is used, and in the case of more than six stations, the least-squares fitting of the quadratic surface with eq (5) is used. When the least-squares fitting of the quadratic surface is used, arithmetic means of available data from the surrounding stations are given to the missing station as temporary values before the surface fitting to balance the distribution of stations. The interpolated stations may be used as surrounding stations in a subsequent interpolation at other stations.

After the first interpolation is completed, another scan is made to reinterpolate wind data at the interpolated stations. In this process of reinterpolation, the data available after the first interpolation are utilized.

Estimate of Divergence by Optimizations 1 Through 4

The divergence, $\nabla\cdot\mathbf{V}$, is evaluated at each station of the synoptic network at each isobaric surface of wind observation by the least-squares fitting of the quadratic and plane surfaces from eq (5) and (6). For the purpose of smoothing the wind field, only the least-squares fitting of polynomial surfaces is performed to compute $\nabla\cdot\mathbf{V}$; the exact fitting is avoided in this step. By having $P(\lambda,\phi)=u$, we obtain $\partial u/\partial\lambda$ from the coefficients of eq (5) and (6); by having $P(\lambda,\phi)=v\cos\phi$, we obtain $\partial(v\cos\phi)/\partial\phi$. When the wind data are not available at a station, or the total number of data stations, including those at the center and those surrounding it, is less than four, $\nabla\cdot\mathbf{V}$ is not evaluated for that station. When the total number of available stations is less that seven, only the plane surfaces are fitted, and, when the total available stations is seven or more, both the quadratic and plane surfaces are fitted.

The divergence estimates for optimizations 1 and 2 are obtained respectively from the quadratic and plane surface fittings using only the observed data. Optimizations 3 and 4 are found by including the interpolated wind data for missing stations in the quadratic and plane surface fittings. With optimizations 1–4, no smoothing of the obtained divergence values is performed.

Estimate of Divergence by Optimizations 5 Through 8

After $\nabla\cdot\mathbf{V}$ values are computed over all possible stations in the network with optimizations 1–4, a space smoothing of the divergence is performed by averaging the $\nabla\cdot\mathbf{V}$ value of a station and the arithmetic mean of the $\nabla\cdot\mathbf{V}$ values of surrounding stations. As the process is repeated for $\nabla\cdot\mathbf{V}$ values computed separately by optimizations 1–4, it will result in $\nabla\cdot\mathbf{V}$ values with optimizations 5–8.

Estimate of Divergence by Optimizations 9 Through 12

Optimizations 9–12 are obtained by separately applying the space smoothing to $\nabla\cdot\mathbf{V}$ values from optimizations 1–4 by the least-squares fitting of the plane surface with eq (6). If fewer than four $\nabla\cdot\mathbf{V}$ values are available at a particular level for the total of that particular station and its surrounding stations, the smoothing is not done.

Selection of ω Profile from Optimizations 1 Through 12

Using $\nabla\cdot\mathbf{V}$ values computed by different optimizations, one can obtain up to 12 ω profiles at each station. Two criteria are used for the selection of an ω profile for individual stations; they are the convergence of the profile at the top of the atmosphere and the bulging of the profile in the midtroposphere. The convergence of the ω profile to a near-zero value is commonly recognized as the most sensitive indicator for the quality of the ω profile. The bulging of the profile in the middle troposphere is used as an auxiliary criterion, because the vertical p velocity is

usually at its maximum in the middle troposphere unless the station is located at a boundary between areas of upward and downward motions. We have observed that, if an oversmoothing of divergence occurs, it often results in the flattening of the ω profile in the middle troposphere. Adoption of these two criteria was based on discussions of the general shape of ω profiles and their space distribution by Knighting (1960), Kung (1972), Smith (1971), Schmidt and Johnson (1972), and Stuart (1964).

Selection of the ω profile is performed at individual stations. First, all computed ω profiles at a station are examined for their general shape. All profiles with absolute values of ω from 250 to 50 mb either greater than 0.4 μb/s or greater than one-third of the absolute value of ω at 500 mb are rejected. The absolute value ratio of an average ω between 200 and 40 mb to an average between 600 and 300 mb is then determined for the remaining profiles. The maximum of the midtropospheric bulge may occasionally occur below the 600-mb level. However, the average ω between 600 to 300 mb, as used in this scheme still may function satisfactorily as a parameter to check midtropospheric ω against the upper level ω. After the comparison, the profile with the smallest absolute value ratio is then selected as the ω profile for that station. In this case, no further computation with optimizations 13 and 14 will be done.

If no profile is selected because of prescribed rejection criteria in the preceding procedure, all profiles of the station are reexamined to determine a profile with the smallest absolute value of the averaged ω from 250 to 50 mb. This profile will be compared with two additional profiles computed with optimizations 13 and 14.

Either way, with this step, a final selection of a profile is made or a tentative selection for a further comparison is made. The $\nabla\cdot\mathbf{V}$ values of a particular optimization that produced the selected ω profile are designated as the divergence at the station for further computation with optimizations 13 and 14.

Estimate of Divergence by Optimizations 13 and 14

A scan is made over the network, and $\nabla\cdot\mathbf{V}$ values by optimizations 13 and 14 are computed for those stations where the final selection of the profile has not yet been made. Divergence by optimization 13 is obtained by averaging the selected $\nabla\cdot\mathbf{V}$ value of the station and the arithmetic mean of those values at surrounding stations; $\nabla\cdot\mathbf{V}$ by optimization 14 is obtained by the least-squares plane surface fitting of the selected $\nabla\cdot\mathbf{V}$ values at the station and the surrounding stations with eq (6).

Two ω profiles with $\nabla\cdot\mathbf{V}$ values by optimizations 13 and 14 and the tentatively selected ω profile in the preceding step are compared at those stations, and a profile with the smallest absolute value of averaged ω from 250 to 50 mb is selected as the ω profile for the station.

The 14 degrees of optimization provided in the scheme according to the preceding description may be summarized in table 1 as 14 methods to compute devergence with the same set of upper air network data.

FIGURE 1.—Distribution of ω profiles over North America at 1200 GMT, July 2, 1962.

TABLE 1.—*Fourteen methods of estimating divergence in optimizing the computation of ω profiles*

Method	Degree of polynomial surface fitting for wind field	Interpolation of missing wind data	Space smoothing of divergence fields
1	Quadratic	No	No
2	Plane	No	No
3	Quadratic	Yes	No
4	Plane	Yes	No
5	Quadratic	No	*
6	Plane	No	*
7	Quadratic	Yes	*
8	Plane	Yes	*
9	Quadratic	No	†
10	Plane	No	†
11	Quadratic	Yes	†
12	Plane	Yes	†
13	(Selected $\nabla\cdot\mathbf{V}$ values from optimizations 1–12 are used for space smoothing.)		
14			†

*Take an arithmetic mean from the surrounding stations and then average with the computed value for the station.
†Least-squares plane surface fitting of the divergence field with $\nabla\cdot\mathbf{V}$ values for the station and surrounding stations

3. APPLICATION OF THE SCHEME OVER AN UPPER AIR NETWORK

As an illustration, the foregoing 14-degree optimization scheme is applied over the North American upper air network. The data source is the Massachusetts Institute of Technology General Circulation Data Library (National Science Foundation Grants GP–820 and GP–3657). Wind observations are used at every 50-mb level from the surface to 100 mb, and at 70 and 50 mb. For the layout of the station network and the use of surrounding stations for polynomial surface fitting, see Kung (1972).

Figure 1 displays ω profiles obtained over the network for 1200 GMT, July 2, 1962, through the depth of the

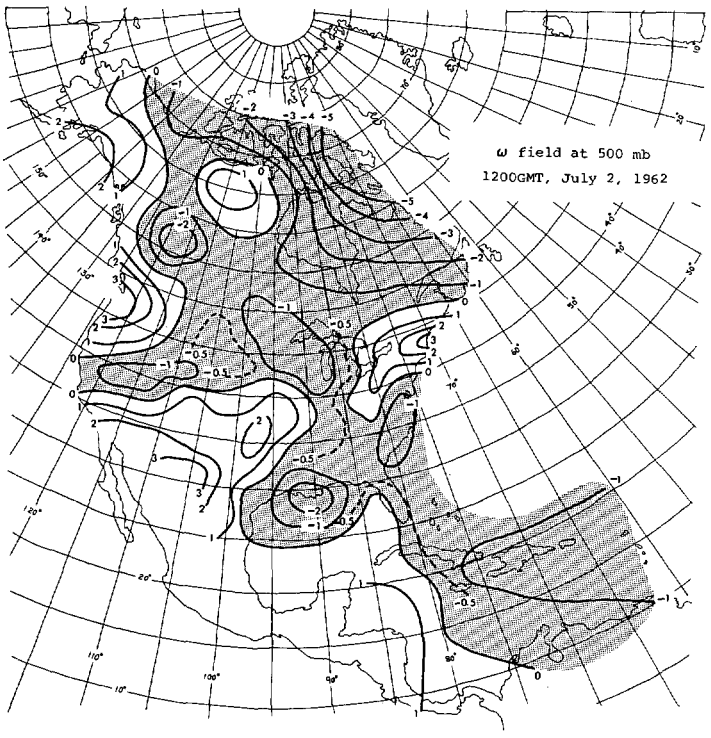

FIGURE 2.—The 500-mb vertical motion field, ω (μb/s), over North America at 1200 GMT, July 2, 1962.

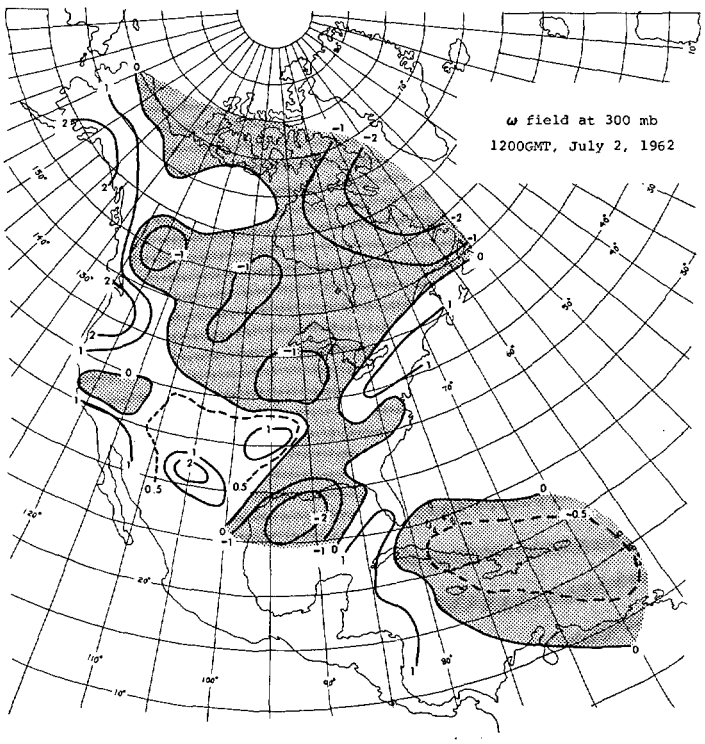

FIGURE 3.—Same as figure 2 for 300 mb.

atmosphere. This choice of day and time was arbitrary. Only those converging profiles are presented and some converging profiles have even been omitted from the figure to avoid a cluttered illustration. An extensive check with other synoptic observation times confirms that the display in the figure represents the normal pattern of the computational results with the 14-degree optimization scheme. The general trend of the convergence of ω profiles at the top of the atmosphere is obvious.

Since ω is computed through the depth of the atmosphere, a synoptic map of ω may be constructed at any pressure level up to the highest level of wind observations. As an illustration, ω maps at 500-, 300-, and 200-mb levels are constructed in figures 2–4, respectively, from the synoptic distribution of ω profiles as presented in figure 1. Figures 5 and 6 are presented to describe the synoptic pattern over North America for the time the vertical motion fields are computed. Surface isobars in figure 5 and 500-mb contour lines in figure 6 were taken from the Daily Series, Synoptic Weather Maps of the National Oceanic and Atmospheric Administration (NOAA). The precipitation pattern for the 24- to 48-hr period in figure 5 was composed from the same source. In the United States and southern part of Canada, the area of precipitation during the 24 hr ending at 0600 GMT on July 3 is indicated by the shaded area; for the rest of Canada and Alaska the shaded areas indicate the precipitation as shown on the 1800 GMT surface maps of July 1, 2, and 3. Comparing the vertical motion fields as illustrated in figures 2–4 with the synoptic patterns as described in figures 5 and 6, we may easily conclude that the magnitude and spatial distribution of the ω values are consistent with the implied pattern of convergence and divergence and also with the precipitation patterns indicated.

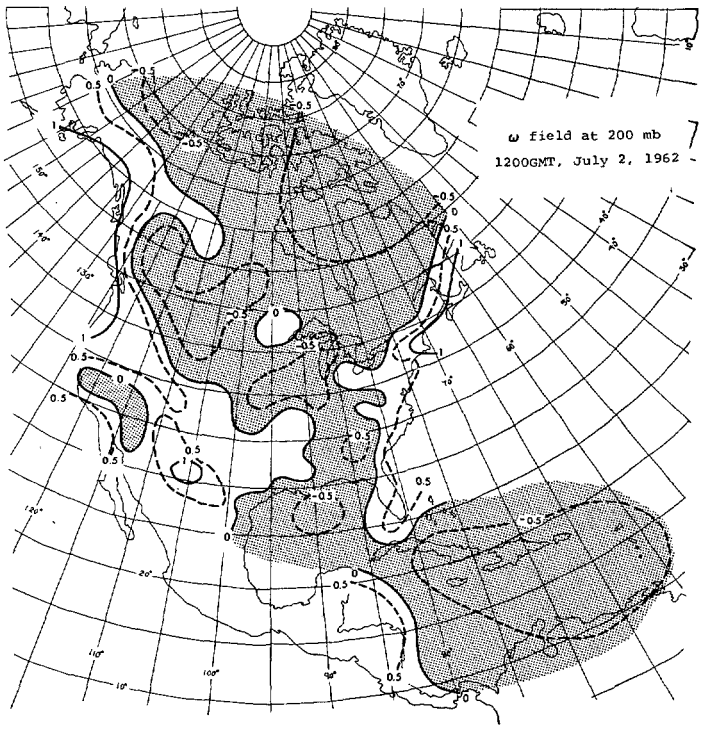

FIGURE 4.—Same as figure 2 for 200 mb.

With the existing mathematical or statistical techniques, it is not particularly difficult to analyze the observed data to describe, smooth, or interpolate the meteorological field. However, the analyzed fields often reveal their weakness when they are further used to compute the higher order parameters, which are generally sensitive to bias errors of various sources. In the case of kinematic vertical velocity, the bias errors contained in the estimated

FIGURE 5.—Surface pressure (mb) and precipitation patterns over North America at 1200 GMT, July 2, 1962. Areas of precipitation during the 24- to 48-hr period are shown by the shaded area.

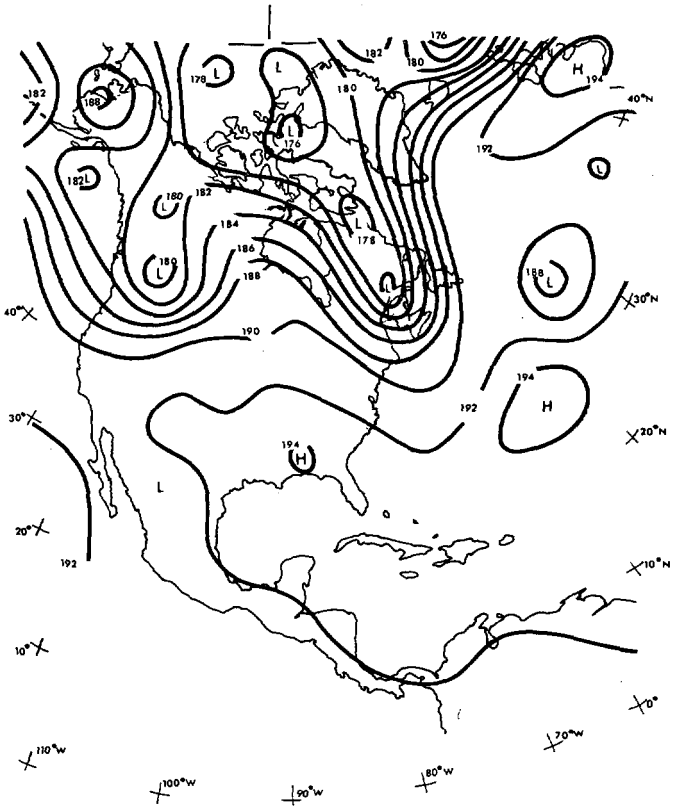

FIGURE 6.—The 500-mb height (10^2ft) over North America at 1200 GMT, July 2, 1962.

divergence usually show up as the nonconverging ω profiles after the vertical integration where the bias errors cannot be eliminated but are accumulated. The degree of uniform convergence of the ω profile and the consistency of profiles with each other and with the synoptic pattern can thus be taken as indicative of the usefulness of the computed ω fields. Indeed, in forthcoming separate papers, the kinematic ω field by this scheme is used to evaluate energetics parameters that will indicate the validity of the scheme. It is pertinent to point out that the ω profiles are computed at individual stations and can be treated as any other meteorological parameter observed at the station for further computational use.

The divergence field and, hence, the consequent vertical motion field, is scale-dependent. Two factors in this regard may be considered concerning the ω values obtained with this optimization scheme. First, the density of the upper air network is different from place to place, thus influencing the scale represented by those ω profiles. For example, the Canadian and Caribbean networks are much less dense than the United States network. Second, a certain degree of difference in the area represented by each profile may exist under different optimizations, since the different optimizations may use different surrounding stations as well as different degrees of space smoothing. The first factor is a problem inherent in any analysis scheme that utilizes the synoptic network data for input. For the second problem, we observed that during our analysis experiment ω profiles at a station converging with different optimizations do not differ appreciably in magnitude. This also may be observed from examples presented in our previous report (Kung 1972). This indicates that the possible variation in the area covered under different optimizations in this scheme does not materially affect the representative ω values in the synoptic scale range.

Although most of the ω profiles over the network indicate the trend of convergence and approach very small values in comparison with those values in the middle troposphere, the computational scheme itself does not require them to be zero at the upper boundary. As a matter of fact, the values obtained at the highest level, 50 mb, still describe a meaningful synoptic pattern. Nevertheless, in the upper levels (namely, above 200 mb or so), the decrease of available wind observations may result in some cases of poor estimates of divergence and consequently a number of nonconverging ω profiles. Taking an example from the same 1200 GMT, July 2, 1962, synoptic time as a typical case, we can make some relevant comments concerning the handling of the problem. In the original data set, 97 of 129 stations in the network area have wind data available up to the 200-mb level; 78 of them extend farther to 100 mb and 61 to 50 mb. This count does not include an extra 23 stations outside the continental boundary that are used only as surrounding stations. After the computation, 119 ω profiles are obtained over the network, which means there are 22 more stations with the ω profile than with the originally available wind profiles due to the interpolation of missing wind data in the

process. Among those 119 computed ω profiles, 13 profiles do not show a trend of convergence and are eliminated as erroneous cases, leaving 106 profiles as useful. Obviously, 106 converging profiles are more than 97 original wind stations and the construction of the vertical motion field over the synoptic network area is warranted.

Among those 106 acceptable ω profiles, 18 profiles show one ω or more above 200 mb with spuriously large absolute values; that is, larger than 0.7 μb/s. Those profiles are fairly normal and consistent with others and can be used without any problem up to about the 200-mb level. Above this level, there appear to be two alternatives in handling this group of profiles. The first, and probably the simplest, is to ignore those profiles. After eliminating these profiles, there are still 88 profiles available above the 200-mb level. As the number of original available observations is less than 90 above this level anyway, those profiles remain ample for describing the vertical motion field at those levels and for being utilized for further computations. The second alternative is to apply vertical smoothing to this group of ω profiles. The smoothing as proposed by O'Brien (1970) seems to be useful in this regard. Smith (1971) has extensively utilized O'Brien's correction scheme and has shown that the correction scheme will preserve the basic shape of the ω profile. From our preceding report (Kung 1972), it also may be deduced that O'Brien's scheme is particularly good in the type of correction needed to deal with the problem we have here if we choose to correct rather than eliminate this group of profiles. The correction will be mainly applied at the higher levels and will not materially influence the midtropospheric and lower tropospheric parts of the ω profile. In this case, the ω value at the highest level may be specified by the interpolation from the surrounding stations, which is the only requirement necessary to apply O'Brien's correction scheme. It will be recognized that essentially the same purpose as the space smoothing of the ω field is accomplished by applying the vertical correction to a limited number of ω profiles.

4. REMARKS

In this note, our current 14-degree optimization scheme for the use of the large aerological data network has been utilized to demonstrate the principles involved in the design and use of the scheme. Depending on the types of data, scale of analysis, and size of the network, one can easily modify the design and use of the scheme to suit the particular situation and need.

Our study has indicated that after the wind fields are interpolated at the fixed gridpoints with eq (5) and/or (6), a similar optimization scheme can be applied to compute the ω profiles at the gridpoints with the combination of the observed and interpolated wind data. With the radiosonde data from a very dense network, such as for the subsynoptic scale study (see McInnis and Kung 1972), our recent computational tests indicate that the vertical smoothing of the divergence field shall be integrated to provide necessary degrees of optimization. The degrees of optimization, of course, are not limited to 14. In our study of tropical energy conversion with the western tropical Pacific data, a scheme with 24 degrees of optimization on the basis of permuted use of available surrounding stations has been successfully applied to an original network observation of 11 stations. In general, we note that the number of unacceptable profiles decreases with the increased degree of optimization.

ACKNOWLEDGMENTS

Sally McConnell and Debbie Kliethermes are acknowledged for their technical assistance in preparation of the paper, and Alan Burgdorf for reading the original manuscript.

REFERENCES

Knighting, E., "Some Computations of the Variation of Vertical Velocity with Pressure on a Synoptic Scale," *Quarterly Journal of the Royal Meteorological Society*, Vol. 86, No. 309, London, England, July **1960**, pp. 318–325.

Kung, Ernest C., "A Scheme for Kinematic Estimate of Large-scale Vertical Motion with an Upper-air Network," *Quarterly Journal of the Royal Meteorological Society*, Vol. 98, No. 416, London, England, Apr. **1972**, pp. 402–411.

McInnis, Donald H. and Kung, Ernest C., "A Study of Subsynoptic Scale Energy Transformations," *Monthly Weather Review*, Vol. 100, No. 2, Feb. **1972**, pp. 126–132.

O'Brien, James J., "Alternative Solutions to the Classical Vertical Velocity Problem," *Journal of Applied Meteorology*, Vol. 9, No. 2, Apr. **1970**, pp. 197–203.

Smith, Phillip J., "An Analysis of Kinematic Vertical Motions," *Monthly Weather Review*, Vol. 99, No. 10, Oct. **1971**, pp. 715–724.

Schmidt, Phillip J. and Johnson, Donald R., "Use of Approximating Polynomials to Estimate Profiles of Wind, Divergence, and Vertical Motion," *Monthly Weather Review*, Vol. 100, No. 5, May **1972**, pp. 345–353.

Stuart, David W., "A Diagnostic Case Study of the Synoptic Scale Vertical Motion and its Contribution to Mid-Tropospheric Development," *Journal of Applied Meteorology*, Vol. 3, No. 6, Dec. **1964**, pp. 669–684.

[Received March 2, 1973; revised July 23, 1973]